Structural, electronic and magnetic properties of chalcopyrite magnetic semiconductors: A first-principles study

Silvia Picozzi[a)] and Alessandra Continenza
Istituto Nazionale di Fisica della Materia (INFM), Dipartimento di Fisica, Università degli Studi di L'Aquila, 67010 Coppito, L'Aquila, Italy

Yu-Jun Zhao, Wen-Tong Geng,[b)] and Arthur J. Freeman
Department of Physics and Astronomy and Materials Research Center, Northwestern University, Evanston, Illinois 60208

Stimulated by recent experimental observations of room-temperature ferromagnetism of $Mn_xCd_{1-x}GeP_2$ and $Mn_xZn_{1-x}GeP_2$, we investigate the structural, electronic, and magnetic properties of this class of systems ($II–Ge–V_2$, $II=Zn$, Cd, and $V=As$, P) as a function of Mn concentration and chemical constituents by means of first-principles density-functional-theory-based codes. Our calculations indicate that, for Mn substituting the II element, the antiferromagnetic alignment is the most stable ordering for all the systems studied. For Zn- and Cd-rich systems, the total magnetic moments per Mn atom of the ferromagnetic phase is very close to the ideal value of 5 μ_B, since the Mn $3d$ states in the minority spin channel are nearly empty; on the other hand, for Mn rich compounds, the stronger $p–d$ hybridization lowers the total magnetic moment to about 4.4 μ_B. © *2002 American Vacuum Society.* [DOI: 10.1116/1.1515801]

I. INTRODUCTION

The attractive idea of manipulating the spin of the electron, in addition to its charge, as an additional degree of freedom, has recently stimulated a very strong interest in the field named "spintronics." [1] Within this framework, the discovery of ferromagnetic materials operating at room temperature and with high-thermal equilibrium stability would be a breakthrough in realizing spin-polarized transistors, or integrating spin logic and nonvolatile spin memory in the exciting field of quantum computing. So far, most of the work has been focused on (Ga, Mn)As or (In, Mn)As diluted magnetic semiconductors (DMS), with transition temperatures up to 110 K.[2] However, the main disadvantages of Mn-doped III–V compounds are the limited solubility of magnetic impurities in the semiconducting matrix and the impossibility of independently controlling doping and magnetic properties, being that Mn in III–V compounds is a source of holes and spins at the same time. In the search for new ferromagnetic materials with high Curie temperatures, the chalcopyrites seem to be good candidates; the expected advantage of these systems is that Mn can readily substitute for the type-II cations, as has been demonstrated for $II_{1-x}Mn_xVI$ alloys with x up to 1.0 without defect formation, due to the natural tendency of Mn to adopt a +2 valence state.[3]

Recently, Medvedkin *et al.*[4] reported room-temperature ferromagnetism (FM) in unintentionally highly doped chalcopyrite $Cd_{1-x}Mn_xGeP_2$ ($x \leq 0.53$) which was prepared by deposition of a Mn layer on both a $CdGeP_2$ film and a bulk single crystal followed by a solid state reaction at elevated temperature. Subsequently, Cho *et al.*[5] reported the discovery of a room-temperature FM semiconductor chalcopyrite $Zn_{1-x}Mn_xGeP_2$ with $T_C = 312$ K and a coercivity of 10–50 Oe at 280 K. They also observed that at temperatures below 47 K, a sample for $x=0.056$ showed antiferromagnetism (AFM), i.e., FM was present between 47 and 312 K. It was suggested that helimagnetic MnP clusters may form in the low-T samples, overall leading to an antiferromagnetic behavior. However, the origin of this unusual transition is not yet clear and more experimental work is called for.

Stimulated by these recent experimental works, we performed accurate first principles calculations within density functional theory in the generalized gradient approximation (GGA) for this class of materials, i.e., for $Zn_{1-x}Mn_xGeP_2$, $Zn_{1-x}Mn_xGeAs_2$, $Cd_{1-x}Mn_xGeP_2$, and $Cd_{1-x}Mn_xGeAs_2$, considering Mn substituting the II-column atom. In particular, in Secs. II and III, we report the computational and structural details, respectively; in Sec. IV we discuss the electronic and magnetic properties in terms of density of states, favored spin-configurations, and magnetic moments and in Sec. V we draw our conclusions.

II. COMPUTATIONAL DETAILS

The theoretical framework on which our predictions are based is the spin-polarized density functional theory. Since it was shown that the local-spin density approximation (LSDA) to the exchange-correlation potential in DMS can severely underestimate equilibrium lattice constants and bond lengths between the $3d$ element and the anions,[6] we use the GGA, following the Perdew–Becke–Erzenhof scheme.[7]

Two different *ab initio* codes, namely the $DMol^3$ (i.e., density functional theory for molecules and three-

[a)]Author to whom correspondence should be addressed; electronic mail: silvia.picozzi@aquila.infn.it

[b)]Present address: Fritz-Haber-Institut der Max-Planck-Gesellschaft, Faradayweg 4-6, D-14195 Berlin, Germany.

dimensional periodic solids)[8] and full potential linearized augmented plane wave (FLAPW)[9] methods are used.

An efficient three-dimensional numerical integration of the matrix elements occurring in the Ritz variational method and the choice of localized numerical orbitals, used as basis set, are responsible for the high level of accuracy of the DMol[3] results. Scalar relativistic effects via a local pseudo-potential for all-electron calculations are included in the method.[10] In this work, a double set of numerical valence functions with a local basis cutoff R_c of 9 a.u. is used. The structural degrees of freedom (internal relaxations and lattice constants) are optimized using DMol[3] and the final equilibrium geometry is checked using the FLAPW method.

The FLAPW is one of the most accurate *ab initio* methods, in which there is no artificial shape approximation for the wave functions, charge density, and potential. For all atoms, the core and valence states are treated fully and semi-relativistically (i.e., without spin-orbit coupling), respectively. The muffin–tin (MT) radii for Zn, Cd, Ge, and Mn are set to 2.3 a.u.; 1.8 and 2.0 a.u. are used for P and As, respectively. An energy cutoff of 9.0 Ry was employed for the wave functions expansion in the interstitial region, whereas a 49 Ry cutoff was used for the charge density and potential. The integrations in reciprocal space are performed following both the Monkhorst–Pack scheme[11] (using a set of 8–24 **k** points in the irreducible wedge of the Brillouin zone) and the tetrahedron method.[12]

III. STRUCTURAL DETAILS

Let us first focus on the structural details. According to the Mn electronic configuration ($3d^5 4s^2$), we expect Mn to readily substitute the II element and we therefore considered $Mn_xII_{1-x}GeV_2$ alloys.[13,14]

Recall that the chalcopyrite differs from the zincblende crystal structure by a doubling of the unit cell along a four-fold axis, rendering the system body-centered tetragonal. Through total energy calculations, we fully optimized the $MnGeAs_2$ system, obtaining $a=5.83$ Å, $c/a=1.9\pm0.05$ and $u\sim0.25$. The estimated numerical uncertainty on the η value can be ascribed to the very small effect on the total energy due to the tetragonal deformation (i.e., $\eta=c/2a\neq1$) around the η equilibrium value. Our optimized structural values are in good agreement (within 0.5% on the a lattice constant) with the values predicted by the "conservation of tetrahedral bonds (CTB) plus $\eta=\eta_{tet}$" theory discussed in Ref. 15. In our work, Pauling's tetrahedral radii[16] were chosen as 1.31, 1.48, 1.22, 1.22, and 1.10 Å for Zn, Cd, Ge, As, and P, respectively; the Mn tetrahedral radius, derived from the Mn chalcogenides, is 1.41 Å. With these values, we obtained $a=5.86$ Å and $c/a\sim1.9$. The good agreement for the As-based chalcopyrite suggests that the "CTB plus $\eta=\eta_{tet}$" rule may even hold for the similar P-based $MnGeP_2$ system; we therefore used $a=5.673$ Å, $c/a=1.889$. Regarding the $IIMnGeV_2$ (II=Zn, Cd, and V=P, As) structures,[17,18] we interpolated the lattice constants (a and η) from the experimental values for the pure bulk semiconducting chalcopyrite and the "CTB plus $\eta=\eta_{tet}$" value for $MnGeP_2$ and

TABLE I. Lattice constant a (in Å) and c/a used in this work. The experimental lattice parameters for the pure II–Ge–V$_2$ chalcopyrites are taken form Ref. 15 and references therein. Values for $MnGeP_2$ and $MnGeAs_2$ are obtained from "CTB plus $\eta=\eta_{tet}$" rules, and for $x=0.5$ and 0.25, the value of a and a/c are interpolated linearly from $x=0$ and 1.0.

	$x=0$		$x=0.25$		$x=0.50$		$x=1.00$	
	a	c/a	a	c/a	a	c/a	a	c/a
$Zn_{1-x}Mn_xGeP_2$	5.466	1.961	5.517	1.943	5.569	1.925	5.673	1.889
$Zn_{1-x}Mn_xGeAs_2$	5.672	1.966	5.718	1.948	5.765	1.929	5.858	1.892
$Cd_{1-x}Mn_xGeP_2$	5.740	1.877	5.723	1.880	5.706	1.883	5.673	1.889
$Cd_{1-x}Mn_xGeAs_2$	5.945	1.886	5.923	1.888	5.902	1.889	5.858	1.892

$MnGeAs_2$ (see Table I). This approximation is equivalent to Vegard's law and works well in this system. For instance, it is reported by Medvedkin *et al.*[4] that the lattice constant decreases to 5.7 Å when the Mn concentration becomes greater than Cd, which means x in the range of 50%–53% since the maximum x value is 53% in the experiment. Our interpolated lattice constant at $x=0.5$ is 5.706, which differs from experiment by only 0.4%.

IV. RESULTS AND DISCUSSION

The FLAPW calculated total energy differences between the FM and AFM states of $II_{1-x}Mn_xGeV_2$ (II=Zn or Cd and V=P or As) are shown in Fig. 1 for $x=0.25$, 0.5, and 1. DMol[3] calculated values show a similar trend and are therefore not shown. For the AFM configurations, we consider "spin superlattices" with alternating magnetically ordered layers along the [100] ([001]) direction for $x=0.25$ ($x=0.50,1.0$). The AFM state is lower in energy than the FM state for all systems with different Mn compositions; for $x=0.5$ and $x=0.25$, all the energy differences are in a small range between -20 and -50 meV and are nearly compound
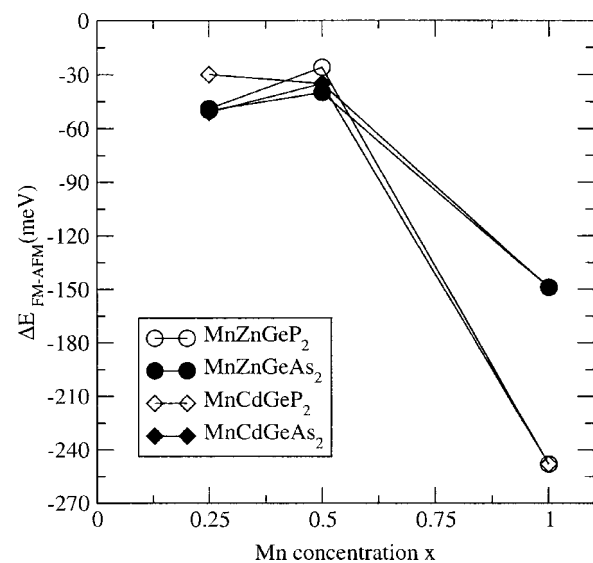

FIG. 1. FLAPW calculated total energy difference (in meV/Mn atom) between FM and AFM states for $Cd_{1-x}Mn_xGeP_2$, $Cd_{1-x}Mn_xGeAs_2$, $Zn_{1-x}Mn_xGeP_2$, and $Zn_{1-x}Mn_xGeAs_2$ as a function of the Mn concentration x.
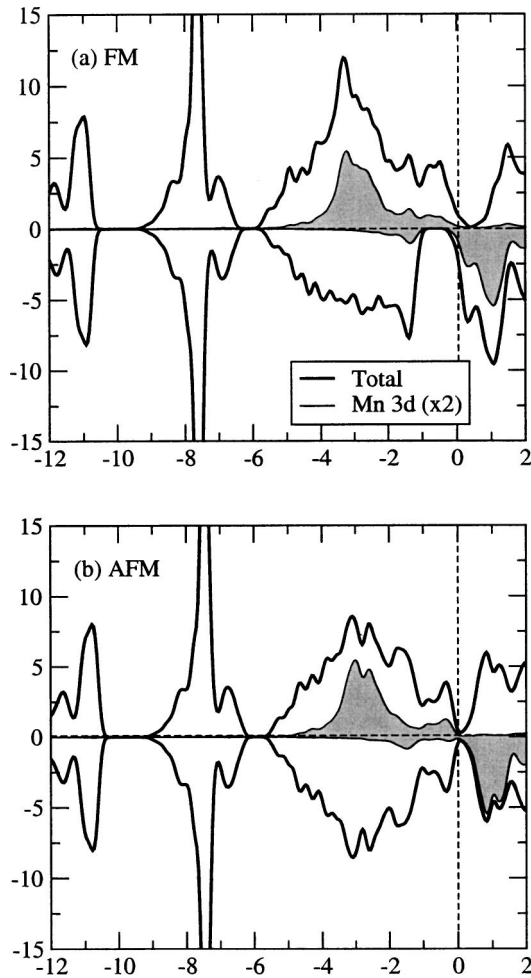
FIG. 2. Density of states for $Zn_{1-x}Mn_xGeAs_2$ for $x=0.5$: the total (bold solid line) and Mn $3d$ (thin solid line) projected density of states are shown for (a) FM and (b) AFM spin configurations. To evidentiate the role of the magnetic impurity in the plot, the Mn $3d$ PDOS was multiplied by a factor of 2.

independent. On the other hand, the effect of the different anion is evident in the $x=1.0$ case, where the P-based compound shows a total energy difference between AFM and FM phases much larger than the As-based compound. Our results

are consistent with those found from first principles in Ref. 13 for Mn-doped $CdGeP_2$: Mn isovalent substitution of Cd site leads to an AFM interaction. For a comparison with experiments,[4,5] showing room-temperature FM, we observe that real samples could be different from our idealized systems, probably exhibiting low-energy hole-producing intrinsic defects,[13] leading to FM.

The total DOS for FM and AFM $Zn_{1-x}Mn_xGeAs_2$ ($x=0.5$) are shown in Fig. 2 as an example; the DOS plots for other systems are very similar.[17,18] For both FM and AFM, the main features are: (i) around -11 eV we find hybridized Ge $s-p$ and anion s bands (ii) around -8 eV we find hybridized Zn d, Ge s, and anion $s-p$ bands; (iii) the states at higher energy (i.e., from -5 to $+2$ eV) have a mixed character. In particular, it is evident that the Mn $d^{\uparrow}$ states are almost totally occupied, whereas the $d^{\downarrow}$ states are mainly unoccupied and hybridized with the p anion states. We can estimate a d exchange splitting of about 4.5 eV.

The FLAPW calculated magnetic properties and the Mn-anion bond lengths are listed in Table II. The calculated Mn–As and Mn–P bond lengths are almost independent of the magnetic ordering at low Mn composition ($x=0.25$), but are slightly shorter in the AFM state for $x=0.5$ and $x=1.0$. For $x\leqslant0.5$, the total magnetic moments for the FM states are very close to the expected value of 5.0 μ_B per Mn since the Mn $3d$ minority states are nearly unoccupied. On the other hand, at $x=1.0$, the free Mn atom magnetic moment (5 μ_B in the d^5 configuration) is reduced due to $p-d$ hybridization, which combines the unoccupied Mn $d^{\downarrow}$ states with the occupied p bands. The total FM magnetic moment of the As-based systems at $x=1.0$ and 0.5 have slightly smaller values than those of P. That is, since As $4p$ states are more delocalized in energy than are P $3p$ states, more Mn $3d^{\downarrow}$ states hybridized with anion p states are occupied in the As systems. The magnetic moment in the Mn muffin–tin spheres are close to 4.0 μ_B in the FM states, but are only 0.04–0.08 μ_B smaller in the corresponding AFM states. This suggests that the spin moments are very localized at the Mn site. The small energy difference between FM and AFM for $x\leqslant0.5$ also suggests that the spin moments are weakly coupled.

TABLE II. FLAPW calculated Mn–anion bond lengths, total magnetic moments, and magnetic moment within the Mn MT sphere in $II_{1-x}Mn_xGeV_2$ for $x=0.25$, 0.5, and 1.0.

| Compound	x	Bond length (Å)		Total moment (μ_B/Mn)		Mn moment (μ_B)	
		FM	AFM	FM	AFM	FM	AFM
$Zn_{1-x}Mn_xGeP_2$	0.25	2.39	2.39	5.00	0	3.83	3.76
	0.50	2.41	2.40	4.99	0	3.89	3.84
	1.00	2.44	2.43	4.37	0	3.80	3.70
$Zn_{1-x}Mn_xGeAs_2$	0.25	2.46	2.46	5.00	0	3.98	3.90
	0.50	2.48	2.47	4.96	0	3.91	3.84
	1.00	2.52	2.51	4.34	0	3.84	3.76
$Cd_{1-x}Mn_xGeP_2$	0.25	2.43	2.43	5.00	0	3.91	3.86
	0.50	2.44	2.43	5.00	0	3.92	3.88
	1.00	2.44	2.43	4.37	0	3.80	3.70
$Cd_{1-x}Mn_xGeAs_2$	0.25	2.50	2.50	5.00	0	3.93	3.88
	0.50	2.50	2.49	4.97	0	3.94	3.88
	1.00	2.52	2.51	4.34	0	3.84	3.76
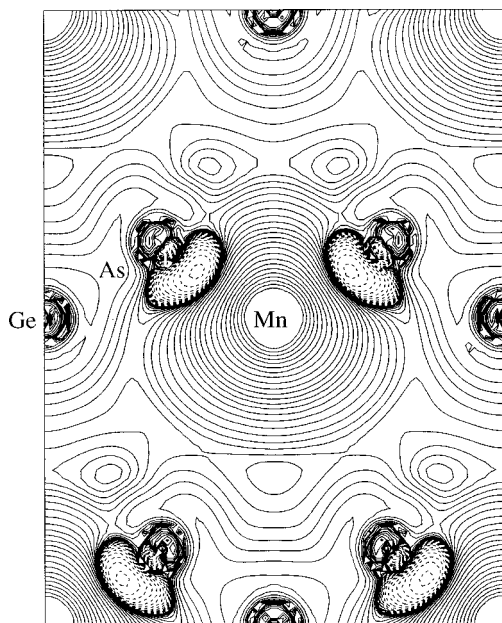
FIG. 3. Spin density of FM $Zn_{1-x}Mn_xGeAs_2$ for $x=0.5$ in the [110] plane. Spin density contours start at 1×10^{-5} and increase successively by a factor of $2^{1/2}$. Positive (negative) spin density is shown by solid (dashed) lines.

Further insights can be gained from the spin-density in FM $Zn_{0.5}Mn_{0.5}GeAs_2$ in the [110] plane, shown in Fig. 3; at variance with the III–V case, the induced spin density is positive around the As atom (resulting in a magnetic moment of about 0.02 μ_B) and in the bond area, even though there is a slightly negative spin-density region along the bond. Our results confirm what was suggested in Ref. 17: with the Mn–anion bond lengths slightly larger in FM than in AFM, the FM Mn–anion interaction seems to be a repulsive effect which increases the total energy, therefore stabilizing the AFM configuration. As a further remark note that small positive magnetic moments are also induced on the Zn (not shown in Fig. 3) and Ge atoms (0.03 and 0.06 μ_B, respectively).

To conclude, all the systems are energetically stable in the AFM phase at $T=0$ K, and the various electronic and magnetic properties are very similar to each other. Being that the Mn valence matched to that of the host substituted atom (i.e., Zn or Cd), there are not hole-like carriers showing up; as a consequence, according to Dietl et al.,[19] we expect that the magnetic properties are nearly independent of the lattice size. This is indeed confirmed by our calculations.

V. CONCLUSIONS

The recently reported room temperature ferromagnetism in $Cd_{1-x}Mn_xGeP_2$ and $Zn_{1-x}Mn_xGeP_2$ stimulated a systematic investigation for this class of compounds, using the FLAPW and $DMol^3$ codes, within the generalized gradient approximation to density functional theory. In particular, we focused on $Cd_{1-x}Mn_xGeP_2$, $Cd_{1-x}Mn_xGeAs_2$, $Zn_{1-x}Mn_xGeP_2$, and $Zn_{1-x}Mn_xGeAs_2$ for $x=0.25$, 0.5, and

1.0 in terms of their structural, electronic, and magnetic properties. We find that the total energy of the AFM state is always lower than the corresponding FM state for all systems studied. The disagreement with experimentally observed room-temperature FM was attributed[13] to hole-producing defects (not considered in our ideally perfect crystals) that may stabilize FM. The total magnetic moment per Mn atom is close to 5 μ_B for the Cd- and Zn-rich systems, whereas it is reduced in the Mn-rich P- and As-based chalcopyrites.

[1] *Diluted Magnetic Semiconductors, Semiconductors and Semimetals*, edited by J. K. Furdyna and J. Kossut (Academic, Boston, 1986), Vol. 25; Y. Ohno, D. K. Young, B. Beschoten, F. Matsukura, H. Ohno, and D. D. Awschalom, Nature (London) **402**, 790 (1999).

[2] H. Ohno, Science **281**, 951 (1998); H. Ohno, J. Magn. Magn. Mater. **200**, 110 (1999).

[3] D. Ferrand et al., Phys. Rev. B **63**, 085201 (2001).

[4] G. A. Medvedkin, T. Ishibashi, T. Nishi, K. Hayata, Y. Hasegawa, and K. Sato, Jpn. J. Appl. Phys., Part 2 **39**, L949 (2000); G. A. Medvedkin, T. Ishibashi, T. Nishi, and K. Sato, Semiconductors **35**, 291 (2001).

[5] S. Cho et al., Phys. Rev. Lett. **88**, 257203 (2002).

[6] A. Continenza, S. Picozzi, W. T. Geng, and A. J. Freeman, Phys. Rev. B **64**, 085204 (2001).

[7] J. P. Perdew, K. Burke, and M. Ernzerhof, Phys. Rev. Lett. **77**, 3865 (1996).

[8] B. Delley, J. Chem. Phys. **113**, 7756 (2000); **92**, 508 (1990).

[9] E. Wimmer, H. Krakauer, M. Weinert, and A. J. Freeman, Phys. Rev. B **24**, 864 (1981), and references therein; **63**, 060101 (2001).

[10] B. Delley, Int. J. Quantum Chem. **69**, 423 (1998).

[11] H. J. Monkhorst and J. D. Pack, Phys. Rev. B **13**, 5188 (1976).

[12] G. Gilat and L. J. Raubenheimer, Phys. Rev. **144**, 390 (1966); O. Jepsen and O. K. Andersen, Solid State Commun. **9**, 1763 (1971); G. Lehmann and M. Taut, Phys. Status Solidi B **54**, 469 (1972).

[13] P. Mahadevan and A. Zunger, Phys. Rev. Lett. **88**, 047205 (2002).

[14] It was pointed out in Ref. 13 that, in the absence of intrinsic defects, the Mn–Cd substitution is favored in a large range of growth conditions. However, chalcopyrites exhibit low-energy intrinsic defects. Therefore, Mahadevan and Zunger showed that, depending on the growth conditions, Mn can even substitute Ge and the interaction between Mn and hole-producing defects could stabilize FM.

[15] J. E. Jaffe and A. Zunger, Phys. Rev. B **29**, 1882 (1984); S. C. Abrahams and J. L. Bernstein, J. Chem. Phys. **59**, 5415 (1973).

[16] L. Pauling, *The Nature of the Chemical Bond* (Cornell University Press, Ithaca, NY, 1967).

[17] Y.-J. Zhao, W. T. Geng, A. J. Freeman, and T. Oguchi, Phys. Rev. B **63**, R201202 (2001).

[18] Y.-J. Zhao, S. Picozzi, A. Continenza, W. T. Geng, and A. J. Freeman, Phys. Rev. B **65**, 094415 (2002).

[19] T. Dietl, H. Ohno, J. Cibert, and D. Ferrand, Science **287**, 1019 (2000).